[20] For an example of a system in which the use of different metal ions leads to changes in cluster stoichiometry and geometry, see reference [17d].
[21] For examples of systems in which slight structural modifications in the ligand changes cluster stoichiometry and geometry, see a) C. Provent, S. Hewage, G. Brand, G. Bernardinelli, L. J. Charbonniére, A. F. Williams, *Angew. Chem.* **1997**, *109*, 1346 – 1348; *Angew. Chem. Int. Ed. Engl.* **1997**, *36*, 1287 – 1289; b) E. J. Enemark, T. D. P. Stack, *Angew. Chem.* **1998**, *110*, 977 – 981; *Angew. Chem. Int. Ed.* **1998**, *37*, 932 – 935.
[22] For examples of solutions containing mixtures of clusters with different stoichiometry and geometry, see a) F. M. Romero, R. Ziessel, A. Dupont-Gervais, A. Van Dorsselaer, *Chem. Commun.* **1996**, 551 – 553; b) P. N. W. Baxter, J.-M. Lehn, *Chem. Commun.* **1997**, 1323 – 1324.
[23] A slightly modified preparation (using $SnCl_2$) based on a literature procedure (M. A. Rabjohns, P. Hodge, P. A. Lovell, *Polymer* **1997**, *38*, 3395 – 3407) was used.
[24] P. F. Schuda, C. M. Botti, M. C. Venuti, *OPPI Briefs* **1984**, *16*, 119 – 123.
[25] SMART, Area Detector Software Package, **1995**, Siemens Industrial Automation, Inc., Madison, WI, USA.
[26] SAINT, SAX Area Detector Integration Program, 4.024, **1995**, Siemens Industrial Automation, Inc., Madison, WI, USA.
[27] G. Sheldrick, SHELXTL Crystal Structure Determination Software Package, **1993**, Siemens Industrial Automation, Inc., Madison, WI, USA.
[28] G. Sheldrick, SADABS, Siemens Area Detector ABSorption Correction Program, Advanced Copy, **1996**; G. Sheldrick, personal communication,
[29] C. S. Pratt, B. A. Coyle, J. A. Ibers, *J. Chem. Soc. A* **1971**, 2146 – 2151.
[30] teXsan, Crystal Structure Analysis Package, **1992**, Molecular Structure Corporation, The Woodlands, TX, USA.

A Simple Lithographic Approach for Preparing Patterned, Micron-Scale Corrals for Controlling Cell Growth**

Pradyut Ghosh, Mary Lee Amirpour, William M. Lackowski, Michael V. Pishko, and Richard M. Crooks*

In this report we demonstrate that a simple, three-step lithographic process—involving microcontact printing (μ-CP), polymer grafting, and subsequent polymer functionalization—results in patterned surfaces exhibiting excellent cell adhesion and spatial definition. The patterned substrates consist of cell corrals having lateral dimensions of 63 μm and wall heights of 54 ± 4 nm. The corrals have hydrophobic, methyl-terminated *n*-alkanethiolate bottoms, which promote cell adhesion, and the walls consist of hydrophilic poly(acrylic acid)/poly(ethylene glycol) (3-PAA/PEG) nanocomposite polymers that resist cell encroachment. Peritoneal IC-21 murine macrophage cell growth occurs only within the boundaries of the corrals. This approach provides a simple and chemically flexible route to local definition of cells on surfaces.

Formation of biological tissue structures, such as nerves and blood vessels, require micron-scale morphologic control and spatial positioning of cells. To achieve this on artificial substrates, the adsorption and adhesion of cells and proteins have been studied on self-assembled monolayers (SAMs) made up of alkanethiolates or alkylsilanes and on thin polymer films.[1–5] There have been a smaller number of studies focused on the adhesion and motility of cells on patterned substrates.[6–11]

Our approach for exerting micron-scale control over cell adhesion involves four steps (Scheme 1).[12] After preparation of a suitable poly(dimethylsiloxane) (PDMS) stamp from a TEM-grid master (TEM = transmission electron microscopy),

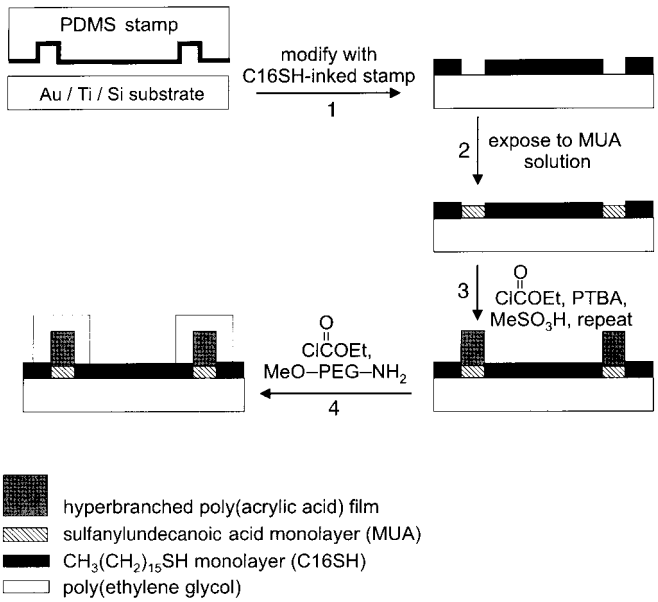

Scheme 1. Formation of micron-scale corrals with hydrophobic alkanethiolate bottoms and walls consisting of a hydrophilic three-layer poly(acrylic acid)/poly(ethylene glycol) nanocomposite.

an evaporated gold substrate is patterned with a hexadecanethiol (C16SH) SAM by soft lithography.[13] Second, the unmodified regions of the gold substrate are filled with a SAM of 11-sulfanylundecanoic acid (also called mercaptoundecanoic acid, MUA). Next, the terminal acid groups of the MUA-patterned portions of the mixed monolayer are activated and treated with α,ω-diamino-substituted poly(*tert*-butyl acrylate) (H_2NR-PTBA-RNH_2) to yield the amide-grafted polymer layer. Hydrolysis of PTBA with $MeSO_3H$ yields the first layer of PAA, and two additional cycles of activation, grafting, and hydrolysis yields a hyperbranched

[*] Prof. R. M. Crooks, Dr. P. Ghosh, Dr. W. M. Lackowski
Department of Chemistry
Texas A&M University
P.O. Box 30012, College Station, TX 77842 – 3012 (USA)
Fax: (+1) 409-845-1399
E-mail: crooks@tamu.edu
M. L. Amirpour, Prof. M. V. Pishko
Department of Chemical Engineering, Texas A&M University
College Station, TX 77843 – 3122 (USA)

[**] This work was supported by the National Science Foundation (CHE-9313441), the Robert A. Welch Foundation, and the State of Texas Higher Education Coordinating Board through the Advanced Technology Program (010366-096) and the Advanced Research Program at Texas A&M University. We thank Prof. David E. Bergbreiter and his research group at Texas A&M University for helpful comments and for providing the α,ω-diamino poly(*tert*-butylacrylate). We also thank Dr. Li Sun (Texas A&M University) for help with the lithography experiments.

  1433-7851/99/3811-1592 $ 17.50+.50/0

three-layer PAA film (3-PAA). The details of this synthesis and the properties of the resulting films have been reported previously.[14] These films contain a high density of acid groups, which can subsequently be functionalized with methoxypoly(ethylene glycol)amine (MeO-PEG-NH_2) by simple amidation chemistry.

Fourier transform infrared – external reflection spectroscopy (FT-IR – ERS), ellipsometry, contact-angle measurements, and X-ray photoelectron spectroscopy (XPS) were performed on macroscopic regions of a partially patterned substrate. This battery of analytical methods confirms that PAA grafting and subsequent functionalization with PEG occurs only on MUA-modified regions of the gold surface. These studies also indicate that covalent attachment of PEG occurs primarily at the surface of the 3-PAA film. For example, the peak at 1730 cm^{-1} in Figure 1a arises from the acid carbonyl group of 3-PAA. After grafting of PEG to the surface, new amide bands appear at 1645 and 1545 cm^{-1} (Figure 1b), but the somewhat diminished acid carbonyl peak remains, indicating only partial derivatization of the 3-PAA film. Exposure of

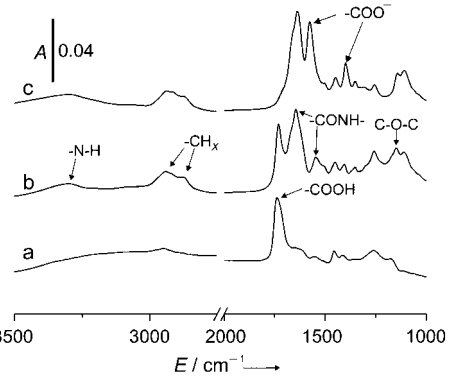

Figure 1. FT-IR – ERS spectra of a) a 3-PAA film; b) the film in a) after derivatization with MeO-PEG-NH_2, immersion into a 0.1M ethanolic solution of HCl to convert unchanged carboxylate groups into the acid form, washing with CH_2Cl_2, and sonication in ethanol to remove physisorbed material from the surface; and c) the film in b) after derivatization with PEG, immersion in aqueous 0.1M CsOH, and rinsing with water and ethanol.

these films to an aqueous CsOH solution resulted in the disappearance of the peak at 1730 cm^{-1} and appearance of new carboxylate peaks at 1580 and 1400 cm^{-1} (Figure 1c), confirming the presence of unfunctionalized acid groups within the interior of the composite. In Figure 1b the presence of a C-O-C stretching band at 1145 cm^{-1}, peaks at 2878 and 2940 cm^{-1} due to the CH_3 and CH_2 stretching modes of PEG, the N–H stretch at 3303 cm^{-1}, and the decrease in the broad OH stretch around 3100 cm^{-1} are additional support for PEG grafting on 3-PAA films. Ellipsometric and tapping-mode AFM mesurements indicate that prior to PEG grafting the 3-PAA film is 23 ± 3 nm thick,[12] but after addition of PEG the composite film thickness increases to 54 ± 4 nm. Additionally, the water contact angle increases from 21° to 27°. Interestingly, there is no change in the water contact angle after soaking of this film in aqueous CsOH solution, even though the film still contains acid groups that have not yet reacted; in the absence of the PEG layer the water contact angle decreases from 21° to less than 5° upon deprotonation of acid groups with CsOH. These results strongly suggest the absence of unchanged acid groups on the surface of the 3-PAA/PEG nanocomposite film. Additional evidence comes from surface-sensitive X-ray photoelectron spectroscopy (XPS) studies of CsOH-treated 3-PAA/PEG films; there is no signal corresponding to Cs, whereas a prominent Cs 3d doublet for PEG-free 3-PAA films appears. Control experiments carried out on a C16SH SAM, rather than on the reactive, acid-terminated MUA monolayer, indicate no growth of PAA and no grafting of PEG.

Prior to cell immobilization all films are sterilized with UV light. Ellipsometry and IR spectroscopy indicate that sterilization does not damage the films chemically or topographically. Figure 2a shows a bright-field micrograph of macrophage cells adhered to an unpatterned hyperbranched 3-PAA film. Adhesion and growth of cells occur because the 3-PAA film contains a high density of acid functional groups. Surface

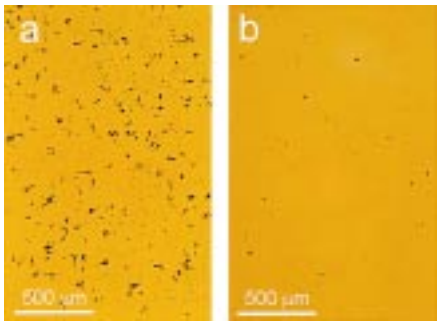

Figure 2. Optical micrographs of macrophage cells seeded onto polymer-modified gold surfaces. a) Adhesion and growth on hyperbranched 3-PAA polymer films grafted onto a self-assembled MUA monolayer. b) Inhibition of adhesion and growth on a 3-PAA film after grafting a layer of PEG to the 3-PAA surface.

sulfonate, hydroxyl, and carboxyl groups have all been demonstrated to promote cell attachment and growth.[15] Figure 2b is an optical micrograph of a 3-PAA/PEG film that was seeded with cells at the same density used for Figure 2a. These data clearly demonstrate that cells neither adhere to, nor grow on, the 3-PAA/PEG films. The absence of cell adhesion on the PEG surface is consistent with the exclusion of protein adsorption, which has been attributed in part to the large excluded volume of PEG chains.[16] These results imply that the relatively thick PEG layer must fully cover the underlying 3-PAA film and that the 3-PAA film, in turn, fully coats the MUA-functionalized gold surface.

Figure 3 shows a bright-field optical micrograph of a square-grid pattern (derived from a TEM-grid master) consisting of C16SH and 3-PAA/PEG on a gold substrate. The grid is a 3-PAA/PEG polymer film and the bottoms of the corrals consist of a C16SH SAM (last frame of Scheme 1).

A micrograph of macrophage cells seeded onto a patterned 3-PAA film is presented in Figure 4a. That macrophage cells grow on both the methyl-terminated SAM and across the 3-PAA corral walls is anticipated by Figure 2a. Figure 4b shows an optical micrograph of a patterned surface in which the corral walls have been modified with PEG. It indicates that PEG inhibits cell adhesion and growth, and that the cells

  1433-7851/99/3811-1593 $ 17.50+.50/0

Figure 3. Optical micrographs of a gold surface patterned using μ-CP followed by polymer grafting. The grid is composed of a 54-nm-thick, PEG-grafted 3-PAA polymer composite, and the squares contain a 1.8-nm-thick *n*-hexadecanethiol (C16SH) monolayer.

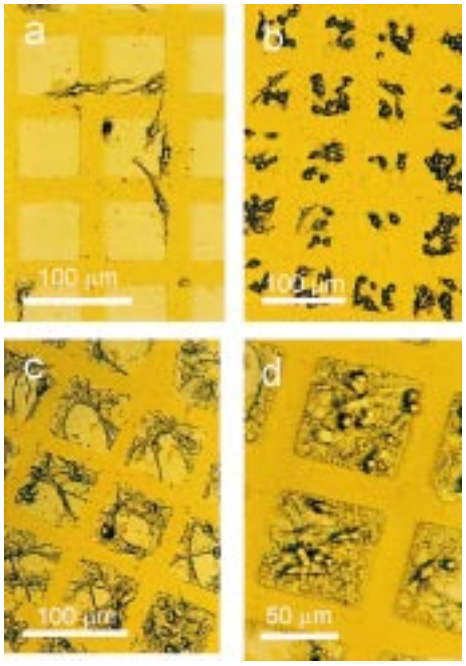

Figure 4. Optical micrographs of a) cells grown onto a patterned film having 3-PAA walls (no PEG) and C16SH bottoms: cells adhere to and grow over the 3-PAA walls; b–d) macrophage cells patterned onto the PEG-modified substrate shown in Figure 3: cells are confined within the corrals, and there is no evidence for cellular interactions between corrals.

are confined to the methyl-terminated SAM surface. These results clearly demonstrate that simple polymer chemistry can be used to control growth; note especially that no part of the cell body escapes the corral. Figures 4c and 4d are higher resolution micrographs of macrophage-patterned regions of the surface. The macrophage cells in these images possess the correct morphology. For example, the peripheral skirt of the cytoplasm and the surface ridges of the cell are evident. Additionally, the cells are well spread, as evidenced by the clearly defined extended processes. Close examination of the macrophage in Figure 4d reveals that it grows only to the boundary of the 3-PAA/PEG corral wall even though the wall is much thinner than the cell. Macrophage cell growth is dependent on the anchorage, so as long as there is surface available the cells will continue to grow. In the case of a fixed area, cell survival is a function of cell-seeding density. At low densities, more surface is available for cell proliferation. We have been able to grow cells for over three days at a density of 1.0×10^4 cells mL^{-1}.

In summary, we have made use of a simple soft-lithography technique and covalent grafting of suitable polymers to prepare micron-scale corrals for cell adhesion and growth. The strict control of cell position and function is a fundamental focus in the development of applications ranging from cellular to tissue engineering,[17] and for biosensing applications. Sequential grafting with polymeric building blocks facilitates a rapid increase in the height of the corral walls, and PEG grafting is so complete that there is no evidence of cell growth outside the corrals. Because the interiors of the corral walls contain unchanged carboxylic acid groups, they can selectively bind metal ions; entrap organic molecules, drugs, and enzymes;[18] or be chemically modified to prevent permeation of aqueous solutions between corrals.[19] Thus, these cell corrals provide new platforms for chemical sensing applications and for tailoring polymer surface properties[20] for a wide variety of biomedical applications. Moreover, this simple patterning strategy may lead to more complex structures such as ensembles of organized tissues, including nerves and blood vessels.

Experimental Section

Methoxypoly(ethylene glycol)amine (MeO-PEG_{5000}-NH_2) was grafted on 3-PAA by immersing the 3-PAA film in 10 mL of dried DMF, to which 200 μL of *N*-methylmorpholine and 200 μL of ethyl chloroformate were added while stirring. After 10 min the substrate was removed, rinsed with ethyl acetate, dried under N_2, and then immersed in a solution of MeO-PEG_{5000}-NH_2 in DMF/CH_2Cl_2 (9/1; 0.1 g of MeO-PEG_{5000}-NH_2 in 9 mL DMF and 1 mL CH_2Cl_2) for 1 h. The slide was then removed, dipped into a 0.1M ethanolic solution of HCl for 10 min to protonate unfunctionalized carboxylate groups and remove salts, dipped in CH_2Cl_2 for 1 h, sonicated in CH_2Cl_2 for 10 min, washed with EtOH to remove physisorbed material from the surface, and finally dried under flowing N_2.

The polymer surfaces were sterilized by placing the substrates under 245-nm UV light for 2 h. SV-40-transformed peritoneal IC-21 mouse macrophages were cultured in RPMI-1640 media supplemented with fetal bovine serum and an antibiotic/antimycotic solution at 37 °C. Cells were plated on supported thin films at a density of 1.0×10^5 cells per mL in all experiments except for cells plated on 3-PAA patterned films (1.0×10^4 cells per mL). After 24 h of incubation at 37 °C in a 5% CO_2 incubator, the substrate-confined cells were put in 10% formalin for 24 h. They were then dehydrated through a series of ethanol washes, treated with hexamethyldisilazane, and imaged by optical microscopy.

Received: November 19, 1998 [Z12685IE]
German version: *Angew. Chem.* **1999**, *111*, 1697–1700

Keywords: biosensors · immobilization · nanostructures · polymers

[1] K. L. Prime, G. M. Whitesides, *Science* **1991**, *252*, 1164–1167.
[2] C. D. Tidwell, S. I. Ertel, B. D. Ratner, B. J. Tarasevich, S. Atre, D. L. Allara, *Langmuir* **1997**, *13*, 3404–3413.
[3] D. A. Stenger, J. H. Georger, C. S. Dulcey, J. J. Hickman, A. S. Rudolph, T. B. Nielsen, S. M. McCort, J. M. Calvert, *J. Am. Chem. Soc.* **1992**, *114*, 8436–8442.
[4] J. G. Steele, G. Johnson, P. A. Underwood, *J. Biomed. Mater. Res.* **1992**, *26*, 861–884.

  1433-7851/99/3811-1594 $ 17.50+.50/0

[5] M. Böltau, S. Walheim, J. Mlynek, G. Krausch, U. Steiner, *Nature* **1998**, *361*, 877 – 879.
[6] S. B. Carter, *Nature* **1965**, *208*, 1183 – 1187.
[7] N. B. Maroudas, *Nature* **1973**, *244*, 353 – 354.
[8] G. P. López, M. W. Albers, S. L. Schreiber, R. Carroll, E. Peralta, G. M. Whitesides, *J. Am. Chem. Soc.* **1993**, *115*, 5877 – 5878.
[9] R. Singhvi, A. Kumar, G. P. López, G. N. Stephanopoulos, D. I. C. Wang, G. M. Whitesides, D. E. Ingber, *Science* **1994**, *264*, 696 – 698.
[10] C. S. Chen, M. Mrksich, S. Huang, G. M. Whitesides, D. E. Ingber, *Science* **1997**, *276*, 1425 – 1428.
[11] D. W. Branch, J. M. Corey, J. A. Weyhenmeyer, G. J. Brewer, B. C. Wheeler, *Med. Bio. Eng. Comput.* **1998**, *36*, 135 – 141.
[12] W. M. Lackowski, P. Ghosh, R. M. Crooks, *J. Am. Chem. Soc.* **1999**, *121*, 1419 – 1420.
[13] Y. Xai, G. M. Whitesides, *Angew. Chem.* **1998**, *110*, 568 – 594; *Angew. Chem. Int. Ed.* **1998**, *37*, 550 – 575.
[14] Y. Zhou, M. L. Bruening, D. E. Bergbreiter, R. M. Crooks, M. Wells, *J. Am. Chem. Soc.* **1996**, *118*, 3773 – 3774.
[15] A. S. G. Curtis, J. V. Forrester, F. Lawrie, *J. Cell Biol.* **1983**, *97*, 1500 – 1506.
[16] S. R. Sheth, D. Leckband, *Proc. Natl. Acad. Sci. USA* **1997**, *94*, 8399 – 8404.
[17] C. S. Chen, M. Mrksich, S. Huang, G. M. Whitesides, D. E. Ingber, *Biotechnol. Prog.* **1998**, *14*, 356 – 363.
[18] J. G. Franchina, W. M. Lackowski, D. L. Dermody, R. M. Crooks, D. E. Bergbreiter, K. Sirkar, R. J. Russell, M. V. Pishko, *Anal. Chem.*, submitted.
[19] M. Zhao, Y. Zhou, M. L. Bruening, D. E. Bergbreiter, R. M. Crooks, *Langmuir* **1997**, *13*, 1388 – 1391.
[20] M. L. Bruening, Y. Zhou, G. Aguilar, R. Agee, D. E. Bergbreiter, R. M. Crooks, *Langmuir* **1997**, *13*, 770 – 778.

Pleated Sheets and Turns of β-Peptides with Proteinogenic Side Chains

Dieter Seebach,* Stefan Abele, Karl Gademann, and Bernhard Jaun

The properties of peptides and proteins depend on their three-dimensional structure, which itself is determined by the sequence of the amino acids, that is, the primary structure. The mechanisms of formation and the parameters determining the stability of secondary structures of proteins—including not only the helix, the pleated sheet, and the turn, but also the random-coiled region—are not yet fully understood.[1] In contrast, β-peptides (oligomers of β-amino acids[2]) adopt predictable[3] secondary structures that can also be identified by calculations.[4] This also holds for β-peptides whose backbones are not conformationally restricted by cyclic residues. Thus, β-peptides composed of more than five homochiral β^2-, β^3-, or *like*-$\beta^{2,3}$-amino acids[5] with proteinogenic side chains form a 3_{14} helix in methanol with all substituents in lateral positions;[3] on the other hand, chains consisting of (*R*)-β^2/(*S*)-β^3 or *unlike*-$\beta^{2,3}$ residues were expected to adopt an extended conformation, with formation of pleated sheets (Figure 1a); in β-peptide sections with (*S*)-β^2/β^3 or with *geminally* disubstituted $\beta^{2,2}$-amino acid moieties we have observed the formation of ten-membered hydrogen-bonded rings (Figure 1b, c). These results and conclusions have provided guidance in our search for β-peptidic parallel and antiparallel pleated sheets and turns, and we have prepared (by known methods[3, 9]) the β-peptides **1** (in solution) and **2** (on solid phase), containing *unlike*-$\beta^{2,3}$-amino acids. Herein, we report their structures.

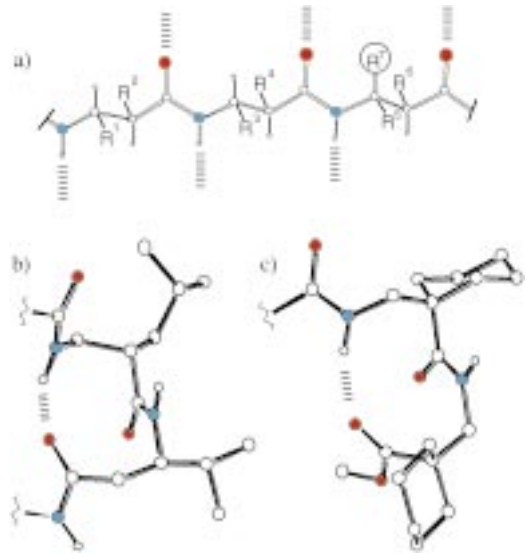

Figure 1. a) Model of a fully extended β-peptide chain. β-Amino acid sequences with R^1 to $R^6 \neq H$, $R^7 = H$ (*unlike*-$\beta^{2,3}$, type I) or, for example, R^1, R^4, $R^5 \neq H$, R^2, R^3, R^6, $R^7 = H$ ((*S*)-β^3/(*R*)-β^2, type II) preclude a β-peptide from adopting the 3_{14}-helical secondary structure; the linear arrangement is enforced.[2, 3, 6] Geminal disubstitution, for example R^5 *and* $R^7 \neq H$, prevents both the formation of the helix and the aggregation to a pleated sheet (see 14-membered hydrogen-bonded turns in Figure 2 and the discussion in reference [3]). b), c) Ten-membered hydrogen-bonded turns found in the β^2-β^3-segments of the 12/10/12 helix[3, 7] or formed by geminally disubstituted β-peptides.[8]

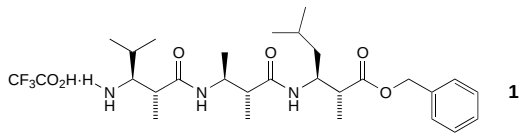

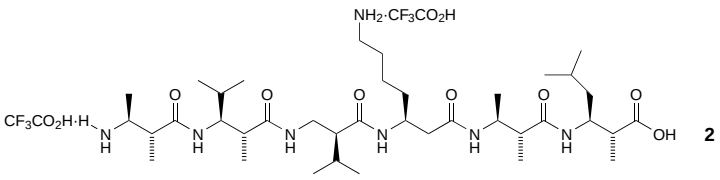

Unsurmountable solubility problems arise upon chain elongation with formation of β-peptides such as **1** (type I in Figure 1a), so that attempted dimerizing coupling of **1** to give a hexapeptide was unsuccessful.[10] The crystal structure and crystal packing of **1**, which indeed forms sheets, are shown in Figure 2.[11] The parallel amide planes in the individual strands

[*] Prof. Dr. D. Seebach, Dipl.-Chem. S. Abele,
Dipl.-Chem. K. Gademann, Prof. Dr. B. Jaun
Laboratorium für Organische Chemie der
Eidgenössischen Technischen Hochschule, ETH-Zentrum
Universitätstrasse 16, CH-8092 Zürich (Switzerland)
Fax: (+41) 1-632-11-44
E-mail: seebach@org.chem.ethz.ch

  1433-7851/99/3811-1595 $ 17.50+.50/0